JOURNAL OF GEOPHYSICAL RESEARCH, VOL. 106, NO. A11, PAGES 24,713–24,731, NOVEMBER 1, 2001

Source of field-aligned irregularities in the subauroral F region as observed by the SuperDARN radars

Keisuke Hosokawa

Department of Geophysics, Graduate School of Science
Kyoto University, Kyoto, Japan

Toshihiko Iyemori

Data Analysis Center for Geomagnetism and Space Magnetism
Graduate School of Science, Kyoto University, Kyoto, Japan

Akira Sessai Yukimatu and Natsuo Sato

National Institute of Polar Research, Tokyo, Japan

Abstract. The HF radars of the Super Dual Auroral Radar Network (SuperDARN) observe the $\mathbf{E} \times \mathbf{B}$ convective drift of ionospheric plasma when suitable small-scale field-aligned irregularities (FAI) from which to scatter are present. In order to estimate the distribution of FAIs in the subauroral F region, we have investigated the scattering occurrence percentage using data from six Northern Hemisphere radars during 39 months between July 1995 and September 1998. We have identified a morphological feature known as the dusk scatter event (DUSE; first reported by *Ruohoniemi et al.* [1988]) in detail and clarified its relation to the boundaries of the plasma density within the subauroral F region. In all months, the DUSE appears within a few hours local time on the eveningside of sunset, where the magnetic latitude is slightly lower than the equatorward edge of the auroral oval, which corresponds to the density-depleted structure known as the midlatitude trough. There exists a clear UT effect in the characteristics of DUSE, such that DUSE is more pronounced for UTs corresponding to dusk on the prime magnetic meridian (0° geomagnetic longitude). Furthermore, an enhancement of scattering occurrence around sunrise within the trough, which is termed dawn scatter event (DASE), was newly identified. The region where the DUSE or DASE occurs has a close relationship with the duskside and dawnside ends of the midlatitude trough in the longitudinal direction (which are termed the sunward edges of the trough in this paper), where sunward directed steep plasma density gradients exist. The Kp dependence of the scattering occurrence was also examined. In disturbed conditions, the DUSE appears at earlier local times compared with that in quiet conditions, which is consistent with the Kp dependence of the sunward edge of the trough. Three models based on the gradient drift instability were discussed. It was found that the model which is based on the sunward plasma density gradient at the sunward edges of the midlatitude trough and ambient electric field is most favorable for the growth of FAIs in this region and can consistently explain the statistical features of DUSE and DASE. These facts indicate that we can estimate the longitudinal extent of the midlatitude trough from the appearance of DUSE and DASE observed by SuperDARN.

1. Introduction

Super Dual Auroral Radar Network (SuperDARN) is an international collaborative project based on the network of coherent HF radars located in the high-latitude zones of the Northern and Southern Hemispheres [*Greenwald et al.*, 1995]. The HF radars of SuperDARN transmit radio waves whose frequency ranges from 8 to 20 MHz. As the waves traverse the E and F regions of the ionosphere, they are scattered backward by the decameter-scale field-aligned irregularities (FAI) when the Bragg condition is satisfied; i.e., significant backscatter is generated only if the radar wave k vector lies in the plane perpendicular to the structure of FAIs.

Paper number 2001JA900080.
0148-0227/01/2001JA900080$09.00

Normally, the radars measure the ionospheric convection velocity by observing the drift motion of these FAIs [*Ruohoniemi et al.*, 1987; *Ruohoniemi and Greenwald*, 1996]. The data of SuperDARN are also useful for the study of FAIs in the high-latitude ionosphere. The scattering occurrence depends on both the existence of FAIs and the conditions of HF wave propagation. Hence the observed "scattering occurrence percentage" is considered to be a lower bound on the actual "occurrence percentage of FAIs," which provides important information about the distribution of FAIs and their generation mechanism.

Recently, several statistical studies of scattering occurrence using SuperDARN have been carried out. *Ruohoniemi and Greenwald* [1997] have investigated the scattering occurrence of 5.5 years of SuperDARN Goose Bay radar observations. In their study, a seasonal variation and a solar cycle dependence of the scattering occurrence are reported. The relationship with the auroral oval and the cusp/cleft region is also discussed. *Milan et al.* [1997] have analyzed the scattering occurrence of SuperDARN Iceland-East and Finland radars statistically. They have shown that FAIs are frequently generated around the dayside cusp/cleft in winter and within the nightside auroral oval in summer. In both papers, however, the occurrence distribution of the FAIs in the subauroral region has not been examined in detail.

Ruohoniemi et al. [1988] had earlier focused on the radar echoes in the subauroral F region and identified a distinctive backscatter feature that appeared in the dusk sector over a period of 5 months centered on winter solstice. This activity, which was called the dusk scatter event (DUSE), was investigated for magnetically undisturbed conditions using the data of SuperDARN Goose Bay radar. They reported that it appears when the solar zenith angle is near 95°. In addition, the source of the DUSE lies in the magnetic latitudes equatorward of the auroral oval (i.e., near the poleward edge of the midlatitude trough). They proposed several mechanisms to explain the enhancement of FAIs in this region. However, the generation mechanism of FAIs responsible for DUSE is still an open question. Moreover, *Ruohoniemi et al.* [1988] did not analyze DUSE during disturbed conditions. The morphological features of DUSE during disturbed conditions should be investigated as well.

In this study we extend the work of *Ruohoniemi et al.* [1988] by analyzing the scattering occurrence percentage of Northern Hemisphere SuperDARN radars statistically. First, we clarify the distribution of subauroral FAIs in each radar and examine whether DUSE is a common feature of all the Northern Hemisphere SuperDARN radars. We also identify a distinctive backscatter feature around sunrise in the subauroral ionosphere, which is termed the dawn scatter event (DASE) in this paper. The seasonal variations of DUSE and DASE in both geographic and magnetic coordinate systems are presented. Especially, we examine the characteristics of DUSE during the period around summer. Finally, we investigate the relationship with the sunward edges of the midlatitude trough for both quiet and disturbed conditions. Consequently, the sources of DUSE and DASE are determined, and a new formation mechanism of FAIs based on the gradient drift instability is proposed.

2. SuperDARN Radars and Statistics Data Set

2.1. SuperDARN Radars

The radars of SuperDARN in the Northern Hemisphere conform to the basic operating design of the first facility which was built at Goose Bay in 1983. A detailed description of the Goose Bay radar has been given by *Greenwald et al.* [1985]. The SuperDARN radars comprise two arrays of log-periodic antennas: one is a main array of 16 antennas with both transmission and reception capability, and the other is an interferometer array of 4 antennas with reception capability only. The radar frequency could be set anywhere from 8 to 20 MHz, but most often it is set between 10 and 15 MHz.

The radars operate on a 24-hour, 365-days-a-year basis, under the control of the operating program. The operation program is separated into three types: common time, special time, and discretionary time. The data used in the statistics are taken from periods when the radars were running in the common time normal scan mode (50% of the whole operation time [see *Greenwald et al.*, 1995]). In the current version of common time normal scan mode the radars carry out azimuthal sweeps through discrete beam pointing directions that are numbered 0-15 with a step in azimuth of approximately 3.2°. It takes approximately 7 s to integrate backscatter returns in one direction, and about 2 min are needed to do a scan of all directions. In general, 75 range gates are sampled for each beam with a pulse length of 300 μs, which is equivalent to a gate length of 45 km, and a lag to the first gate of 1200 μs (180 km). In this configuration the maximum range of the radars is approximately 3550 km. Hence the radar field of view in each scan contains 1200 cells (75 ranges × 16 beams).

2.2. Statistics Data Set

Eight SuperDARN radars are currently under operation in the Northern Hemisphere (their fields of view are shown in Figure 1). The Kodiak and Prince George radars started operation in the beginning of 2000. We used the data from six Northern Hemisphere SuperDARN radars: Saskatoon, Kapuskasing, Goose Bay, Iceland-West, Iceland-East, and Finland (listed in Table 1, shaded fields of view in Figure 1). All data used in the statistics belong to the category of common time normal scan mode. The study period encompassed 39 months from July 1995 to September 1998, which cor-

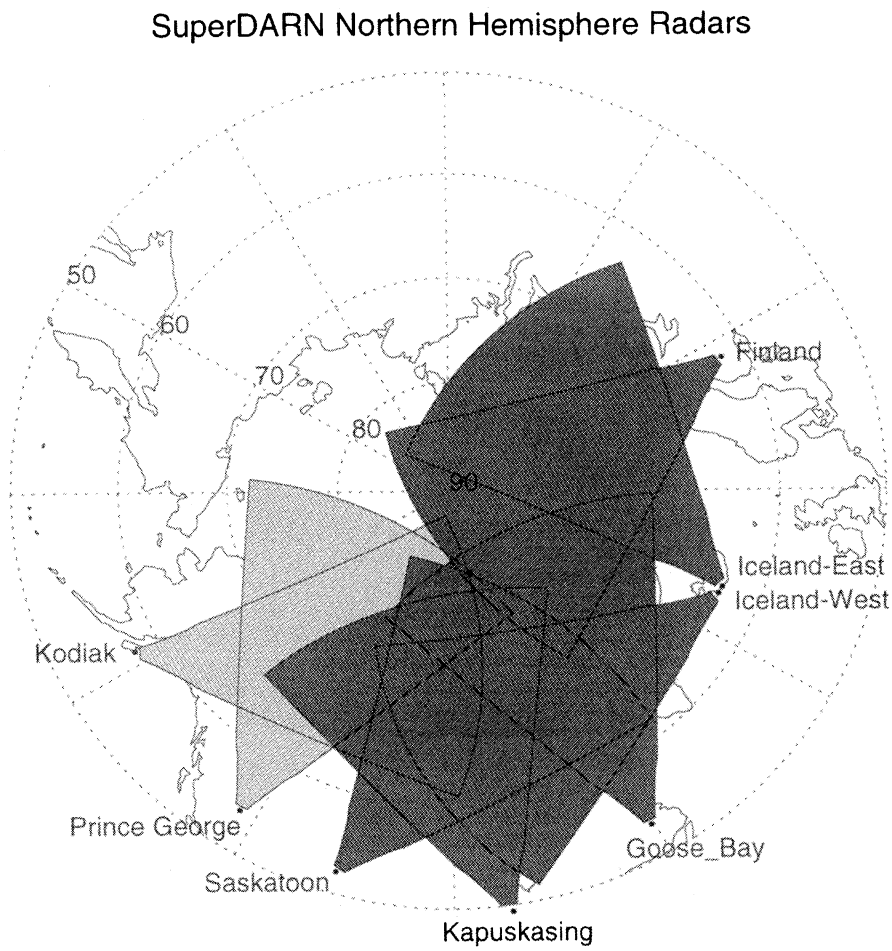

Figure 1. Fields of view of the Northern Hemisphere SuperDARN radars (Kodiak, Prince George, Saskatoon, Kapuskasing, Goose Bay, Iceland-West, Iceland-East, and Finland) in the geographic coordinate system. Shaded fields of view indicate the radars used in the statistics.

responds to the most recent period of solar cycle minimum. All radars except for Iceland-East started operation before July 1995. In the case of Iceland-East, the use of the data is limited to 35 months because this radar has been operational only since mid-November 1995. The number of days used in the statistics is approximately 15 days in each month.

3. Method of the Statistics

3.1. Data Selection

The purpose of this study is to reveal the distribution of FAIs in the subauroral F region. In particular, we aim at a detailed understanding of the morphological feature, the source region, and the formation process of

Table 1. Location and Affiliation of Northern Hemisphere SuperDARN Radars Used in the Statistics

Radar	Affiliation	Geographic Latitude, deg	Geographic Longitude, deg	Start Date
Saskatoon	University of Saskatchewan	+52.16	−106.53	Sept. 1993
Kapuskasing	JHU/APL[a]	+49.39	−82.32	Sept. 1993
Goose Bay	JHU/APL[a]	+53.32	−60.46	June 1983
Iceland-West	CNRS[b]	+63.86	−22.02	Oct. 1994
Iceland-East	University of Leicester	+63.77	−20.54	Nov. 1995
Finland	University of Leicester	+62.32	+26.61	Feb. 1995

[a] JHU/APL, Johns Hopkins University/Applied Physics Laboratory.
[b] CNRS, Centre National de la Recherche Scientifique.

DUSE. Hence we need to deal with reliable echoes from F region FAIs. The main targets of the SuperDARN HF radars are the F region FAIs. The radars, however, also receive backscatter echoes from E region FAIs and from the ground as well as ghost scatter that is due to radio interference. We must exclude these echoes from the scattering occurrence statistics. In the SuperDARN observations, the radar echoes whose range is less than 600 km are regarded as being due to E region scatter, while echoes returned from ranges larger than 900 km are considered to be due to F region scatter [*Ruohoniemi et al.*, 1988]. Hence data obtained from ranges greater than 900 km are taken in the statistics. Echoes that are considered to be ground scatter are excluded on the basis of their line-of-sight velocity magnitude and spectral width (criteria are $V_{\rm los} < 30$ m/s and spectral width of <30 m/s). Finally, we remove the echoes which do not have sufficiently strong signal (< 3-dB signal-to-noise ratio) in order to eliminate much of the ghost scatter due to radio interference. Consequently, we constructed a database of F region FAIs which is largely uncontaminated by E region scatter, interference, or groundscatter.

3.2. Scattering Occurrence Percentage

After the noise reduction process described above, velocity data of the radars are mapped into both geographic (geographic latitude/local time) and magnetic (magnetic latitude/magnetic local time) coordinate systems. Here the Altitude Adjusted Corrected Geomagnetic Coordinates (AACGM) coordinate system (based on the work of *Baker and Wing* [1989]) is used to calculate magnetic latitude and magnetic local time. We sorted the filtered data into 1° × 3° latitude/local time bins, indexed by (i, j), in both coordinate systems for each month period. Then, we can compute the total number of F region scattering, $N_{\rm fai}(i, j)$, and the total number of observation times, $N_{\rm obs}(i, j)$, in each bin. The following formula provides the scattering occurrence percentage, $\Re$, in each coordinate system:

$$\Re = \frac{N_{\rm fai}(i,j)}{N_{\rm obs}(i,j)} \times 100.$$

Plate 1a and 1b show the distribution of the total number of F region scattering, $N_{\rm fai}$, and the total number of observation times, $N_{\rm obs}$, respectively, which are deduced from the data of six Northern Hemisphere radars collected in January between 1996 and 1998. Plate 1c shows the scattering occurrence percentage, $\Re$, calculated by dividing the values of Plate 1a by those of Plate 1b. The scattering occurrence distribution in the magnetic coordinate system is obtained by the same procedure. In the next section, we will show the monthly scattering occurrence percentage in both coordinate systems and discuss the relationship with several boundaries of plasma density in the subauroral F region. As will be described in more detail later, we relate our results to the morphology of the midlatitude trough, whose location depends on solar zenith angle (which is best described in a geographic coordinate system), and the location of the auroral oval (best described in geomagnetic coordinates). For this reason, we find it useful to plot our scattering occurrence statistics in both geographic and geomagnetic coordinate systems.

4. Results of Statistics

4.1. Statistical Signature of DUSE

Plate 2 shows the scattering occurrence percentage mapped into (Plate 2a) a geographic coordinate system (55°-90°) and (Plate 2b) a magnetic coordinate system (65°-90°). These results are deduced from the observation of six Northern Hemisphere radars in January between 1996 and 1998.

In the geographic coordinate system (Plate 2a), two white lines represent the points where the solar zenith angle (SZA) is equal to 90° at the start of the month and the end of the month. A distinct peak in the scattering occurrence (≈25%) is found in the eveningside of dusk as defined by the SZA 90° lines. This peak extends from 1530 LT to 1730 LT (the center of the peak is indicated by a red triangle) and its latitudinal location ranges from 55° to 65°. Another peak is seen around the dawnside SZA 90° lines (indicated by a blue triangle), whose latitudinal location also ranges from 55° to 65°. Its occurrence percentage is, however, smaller (≈7%) in comparison with that in the duskside, which suggests that there exists a marked asymmetry of the FAI occurrence between sunrise and sunset.

In the magnetic coordinate system (Plate 2b), two white circles indicate the equatorward and poleward edges of the auroral oval [*Feldstein and Starkov*, 1967] as modeled by *Holzworth and Meng* [1975] for $Q = 1$ (quiet conditions). A peak of scattering occurrence rate (≈18%) is seen in the dusk meridian between 1500 MLT and 1800 MLT (the center of the peak is indicated by a red triangle). The magnetic latitudes of the peak in the dusk meridian are slightly lower than the equatorward edges of the auroral oval and coincide with the regions of density depletion called the midlatitude trough [*Spiro et al.*, 1978; *Moffet and Quegan*, 1983; *Rodger et al.*, 1992].

Furthermore, a weak enhancement of scattering occurrence (≈4%) is also seen between 0800 MLT and 1000 MLT on the dawnside (indicated by a blue triangle). The magnetic latitudes of the peak are lower than the Feldstein oval; however, there is a little offset between the magnetic latitudes of the dawnside activity and those of the equatorward edge of the oval (about 5° in magnetic latitude). The model of the midlatitude trough by *Collis and Haggstrom* [1988] and the two-dimensional electron density profile reported by *Holt et al.* [1983] suggest that the magnetic latitudes of the midlatitude trough have a dawn/dusk asymmetry (i.e., the latitudes of the dawnside trough are relatively lower in comparison with those of the duskside trough). This

feature of the trough might cause the offset between the latitudes of the dawn activity and those of the Feldstein oval.

Ruohoniemi et al. [1988] reported that DUSE appears when the solar zenith angle ranges between 95° and 105°. It was also pointed out that the source of DUSE lies in the midlatitude trough. The statistical features of the peak in the dusk sector in Plate 2 satisfies these conditions, which means that we can discuss the morphology of DUSE using the statistics of the scattering occurrence. Furthermore, the activity around sunrise (hereinafter called "dawn scatter event" and referred to as DASE) is one of the new results found in this analysis, which has not previously been discussed.

Another clear peak is seen in the local noon sector (0900-1600 MLT) between 76° and 82° latitudes (Plate 2b), which is considered to be associated with the cusp/cleft region and has already been reported by *Ruohoniemi and Greenwald* [1997] and *Milan et al.* [1997]. Radar echoes in this region are characterized by broad Doppler spectral width [*Baker et al.*, 1990, 1995; *Rodger et al.*, 1995; *Yeoman et al.*, 1997; *Milan et al.*, 1998, 1999]. It is worth pointing out that DUSE and DASE are more prominent for mapping in geographic coordinates, while the cusp/cleft scatter feature is more prominent in geomagnetic coordinates. This suggests that the degree of solar EUV influence on DUSE and DASE is stronger than that on the cusp/cleft echoes.

4.2. Feature of DUSE in Each Radar

In the previous section, we have shown that the peak of scattering occurrence, which is regarded as the statistical signature of DUSE, appears around sunset within the midlatitude trough. However, we have not ascertained whether or not this is a common feature among the Northern Hemisphere SuperDARN radars. Here we investigate the scattering occurrence distribution of each Northern Hemisphere radar individually and confirm that DUSE is a reliable feature of F region FAIs that is commonly observed by all radars.

Plate 3 shows the scattering occurrence percentage of each radar in January between 1996 and 1998 as mapped into magnetic coordinate system. Two white lines indicate the Feldstein oval during quiet periods. In all panels, there exists a peak of scattering occurrence around dusk meridian (between 1500 MLT and 1800 MLT; the center of the peak is indicated by a red triangle) outside of the auroral oval, which confirms that DUSE is a common feature of Northern Hemisphere SuperDARN radars. However, the percentage of the peak region is different among the radars. The maximum percentage is obtained in Kapuskasing (≈25%) and the minimum percentage is in Finland (≈15%). The DUSE is more pronounced for Kapuskasing and Goose Bay. Thus there exists a clear UT effect in the characteristics of DUSE, such that the activity of DUSE is more pronounced for universal times corresponding to dusk on the prime magnetic meridian (0° longitude). We can identify the universal times where the activity of DUSE is most intense as a function of season. DUSE is more pronounced during universal times between 0100 and 0300 UT in summer and 2200 and 2400 UT in winter.

There could be several reasons for this dependence. One is an actual UT dependence in the intensity of irregularity formation in the dusk sector, which might be caused by a UT dependence in the background ionization level or convection electric field. Or it might be due to a propagation effect. That is, the raypath or aspect condition is more favorable for the scattering within the subauroral F region in the case of Kapuskasing and Goose Bay, which is probably because the relationship between the magnetic field configuration and vertical plasma density profile is more suitable for scattering in these magnetic longitudes. The geographic latitudes of the Kapuskasing and Finland radars differ by 13° (49.3° versus 62.3°), which suggests that the level of background ionization at dusk will be higher at Kapuskasing. The density gradients associated with solar EUV radiation will also be stronger at Kapuskasing. These differences might cause the UT dependence in the activity of DUSE through their influence on irregularity formation or propagation condition.

Another peak around sunrise, which is identical to DASE, is seen in the Canadian radars (Saskatoon, Kapuskasing, and Goose Bay), the center of the peak being indicated by a blue triangle. On the other hand, non-Canadian radars cannot observe it. Even for the Canadian radars, DASE does not appear until fairly late in the morning, which suggests that it takes a while for background ionization levels or the density gradient to build up to some level in the dawn sector. For the non-Canadian radars, ionization and density gradient might not reached this level in January, which could cause the absence of DASE for them. The Iceland-West radar has echo characteristics different from the other radars. For example, the scattering occurrence is strongly enhanced in the domain poleward of the duskside auroral oval, which is not seen in the other radars. We suppose that this difference is due to the beam direction of Iceland-West. As shown in Figure 1, the Iceland-West radar is directed considerably westward, which may affect the enhancement of scattering occurrence poleward of the auroral oval.

Plate 4 shows range-time-parameter plots of the line-of-sight Doppler velocity observed by the six Northern Hemisphere radars on November 1, 1997. Only the data with backscattered power greater than 3 dB are shown. The gray area indicates ground scatter region. The level of geomagnetic disturbance is relatively quiet during this period (the Kp index ranged from 1+ to 2 over 1200-2400 UT). During this day, all six radars observed the echoes regarded as DUSE, which is enclosed by red rectangles in each panel. DUSE in Plate 4 present the clearest example from the period of our study. The UT of the DUSE increased systematically with increasing westward longitude beginning with

Finland radar. The Canadian radars (Saskatoon, Kapuskasing, and Goose Bay) observed the clear signature of DASE, which is enclosed by blue rectangles. Iceland-East and Finland radars also observed some dawn activity regarded as DASE around 0800 UT. However, the signature of DASE in Iceland-East and Finland is rather weak, which is not intense enough to be identified in our statistical analysis. The UT of the DASE also increased from Finland to Saskatoon with increasing westward longitude. These characteristics of DUSE and DASE agree with the statistical results shown in Plate 3. After all, the signature of DUSE and DASE in our statistics is most clearly seen in the Canadian radars (Saskatoon, Kapuskasing, and Goose Bay). After this, we discuss the scattering occurrence statistics deduced from the Canadian radars.

4.3. Seasonal Variation of DUSE

All statistical results presented in the previous section are derived from the observations in winter. The morphological characteristics of DUSE during winter have already been investigated by *Ruohoniemi et al.* [1988] in detail. They, however, did not detect DUSE during summer; so the morphology of DUSE during summer should be examined. In general, the midlatitude trough in the dusk sector extends equatorward with increasing local time in accordance with the motion of the auroral oval [*Collis and Haggstrom*, 1988; *Rodger et al.*, 1992; *Hargreaves and Burns*, 1996]. Thus the cross section of the midlatitude trough at sunset also moves equatorward during summer, which could be the reason why SuperDARN Goose Bay radar cannot observe DUSE in summer [*Ruohoniemi et al.*, 1988]. Here we present the monthly scattering occurrence distribution deduced from the Canadian radars and clarify the seasonal variation of DUSE. Since the fields of view of Saskatoon and Kapuskasing radars are located at slightly lower latitudes than the radar field of view of Goose Bay, it is expected that the signature of DUSE may be found even in summer.

Plate 5a shows the maps of monthly scattering occurrence percentage as a function of geographic latitude and local time, which are derived from the data of Canadian radars. As noted above, two white lines represent the points where the solar zenith angle is equal to 90° at the start of the month and the end of the month. The scattering occurrence percentage peaks in the lower-latitude region within a few hours of local time on the eveningside of the SZA 90° lines. This tendency is found throughout the year, and the peak moves with the SZA 90° lines month by month. Scattering occurrence percentage in this area reaches its maximum in both winter and summer (≈25%), with a minimum in spring (≈17%). The occurrence of DUSE is rivaled only by that of the cusp/cleft feature in winter, which indicates that DUSE is one of the most reproducible features of the radar observations. The latitudinal width of the peak region is large in winter (from 55° to 70°) and small (from 55° to 62°) in summer. On the other hand, the longitudinal scale is wide in summer and narrow in winter. During winter months (November, December, and January) there is a weak enhancement of scattering occurrence, whose occurrence rate is less than 7%, around the SZA 90° lines between 0800 LT and 1000 LT.

Plate 5b shows maps of monthly scattering occurrence rate as a function of magnetic latitude and magnetic local time, which is deduced from the same data set as that used in Plate 5a. In all months, a clear peak of scattering occurrence is seen in the dusk meridian whose magnetic latitude is slightly lower than the equatorward edge of the auroral oval. These peak regions are considered to be the same as those seen around sunset in the geographic coordinate system. In addition, a weak peak of scattering occurrence is also seen in the dawnside around 0900 MLT in the winter months. Overall, we find that the characteristics of DUSE in summer are the same as those in the other seasons; i.e., the statistical signature of DUSE is located on the eveningside of the SZA 90° lines within the midlatitude trough throughout the year.

4.4. Relationship With the Sunward Edge of Trough

Our statistical analysis confirmed the basic feature of DUSE reported by *Ruohoniemi et al.* [1988], especially the relationship between DUSE and the latitudinal location of the midlatitude trough. The midlatitude trough is primarily a nightside phenomenon, though it extends into the dawn and dusk sectors [*Rodger et al.*, 1992]. *Halcrow and Nisbet* [1977] investigated the data from low-altitude satellites and reported that the duskside and dawnside ends of the midlatitude trough in the longitudinal direction (hereinafter this boundary is termed the sunward edge of the trough) are controlled by the solar zenith angle and geomagnetic disturbance level as estimated by the Kp index. They constructed a model of the sunward edge of the midlatitude trough as a function of solar zenith angle and Kp index. At the sunward edge of the trough, there exists a steep plasma density gradient directed sunward.

Whalen [1987, 1989] also detected the longitudinal extent of the midlatitude trough using the global ionosonde network and clarified where the sunward edge of the trough is located, obtaining basically the same results as *Halcrow and Nisbet* [1977]. *Sojka et al.* [1990] also demonstrated that the longitudinal extent of the midlatitude trough is controlled by the solar radiation and magnetic activity using their time-dependent ionospheric model (TDIM). In the following, we shall pay attention to the sunward edge of the midlatitude trough and investigate its relationship with DUSE and DASE, which was not considered by *Ruohoniemi et al.* [1988]. Here we employ the model of *Halcrow and Nisbet* [1977] and compare the areas where DUSE and DASE occur with the sunward edges of the midlatitude trough.

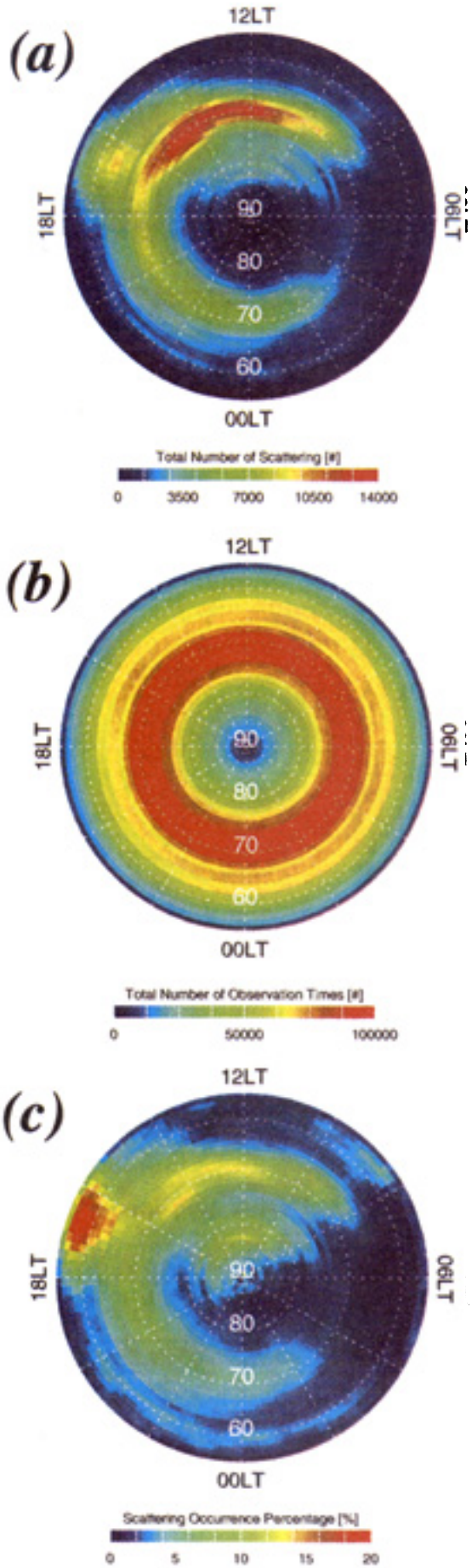

Plate 1. (a) Total number of F region scattering in January between 1996 and 1998 as mapped into the geographic coordinate system. (b) Total number of observation times during the same period as Plate 1a. (c) Scattering occurrence percentage obtained by dividing values of Plate 1a by those of Plate 1b.

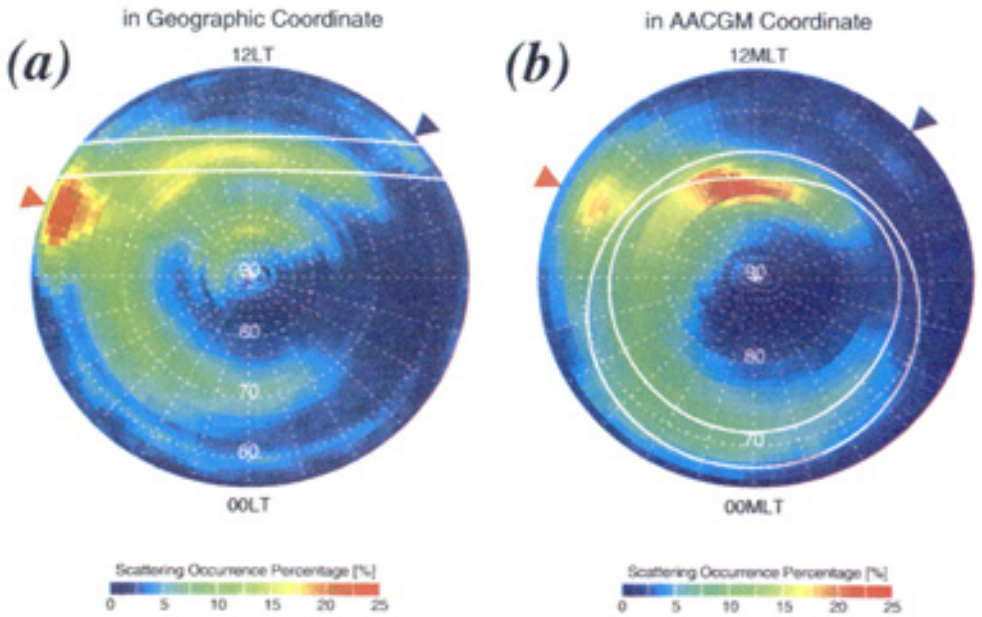

Plate 2. Scattering occurrence percentage of all six radars in January between 1996 and 1998: (a) as mapped into the geographic coordinate system and (b) as mapped into the magnetic coordinate system (AACGM coordinates). In Plate 2a, two white lines represent the points where the solar zenith angle is equal to 90° at the start of the month and the end of the month. In Plate 2b, two white circles indicate the equatorward and poleward edge of the auroral oval [*Feldstein and Starkov*, 1967] as modeled by *Holzworth and Meng* [1975] for $Q = 1$ (quiet conditions).

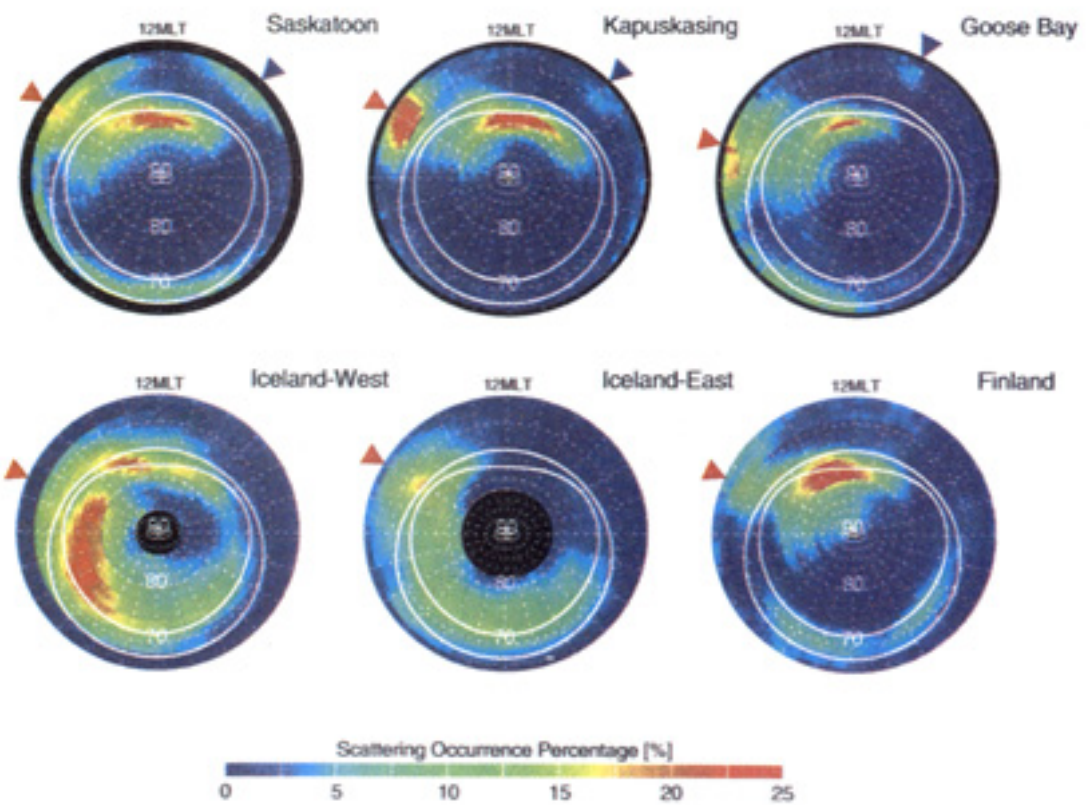

Plate 3. Scattering occurrence percentage of each radar in January between 1996 and 1998 as mapped into the magnetic coordinate system. Two white lines indicate the poleward and equatorward edge of the Feldstein oval as before.

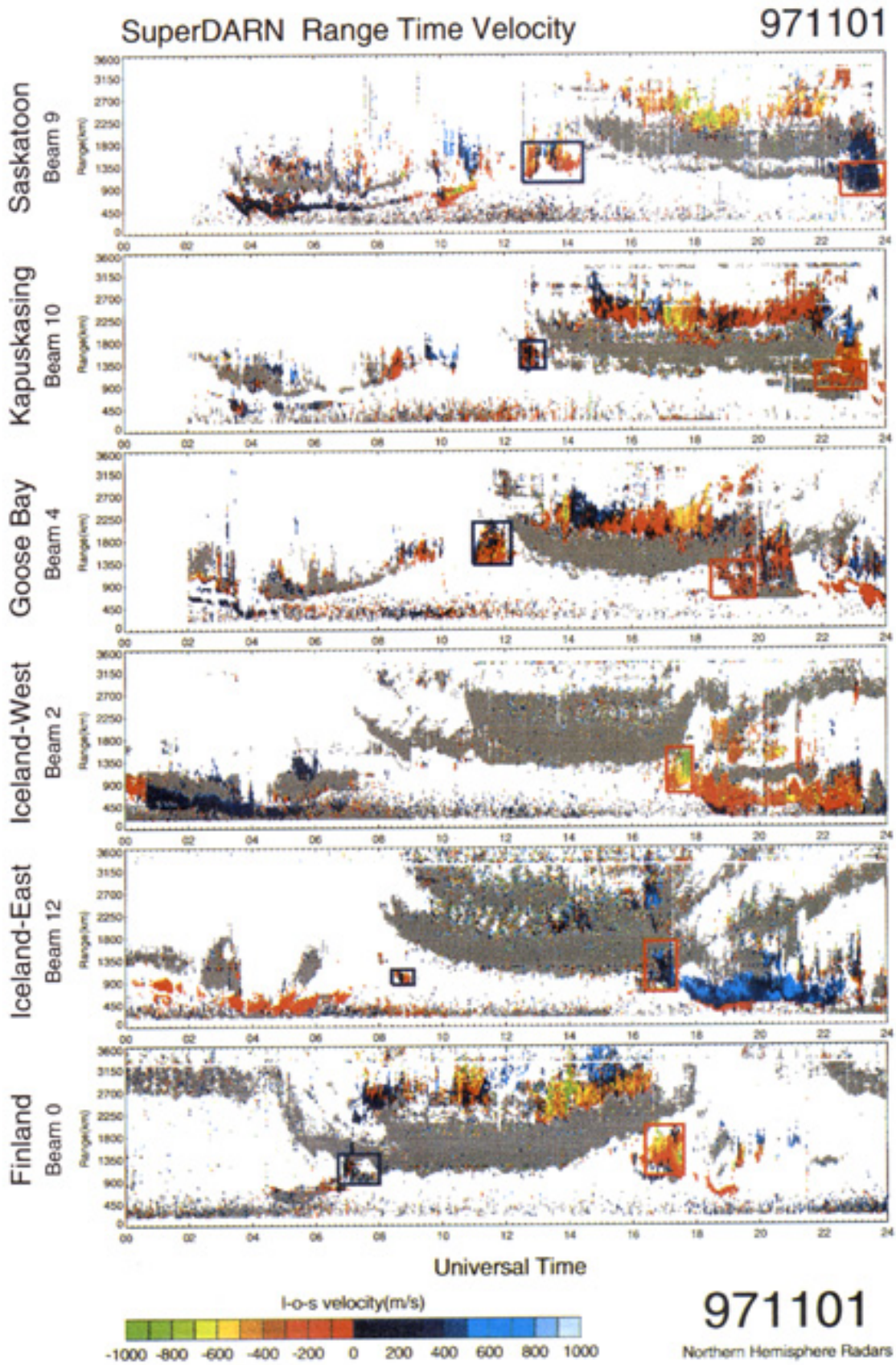

Plate 4. Range-time-parameter plots of line-of-sight Doppler velocities observed by the six Northern Hemisphere radars on November 1, 1997. DUSE is indicated by a red rectangle in each panel, and DASE is indicated by a blue rectangle.

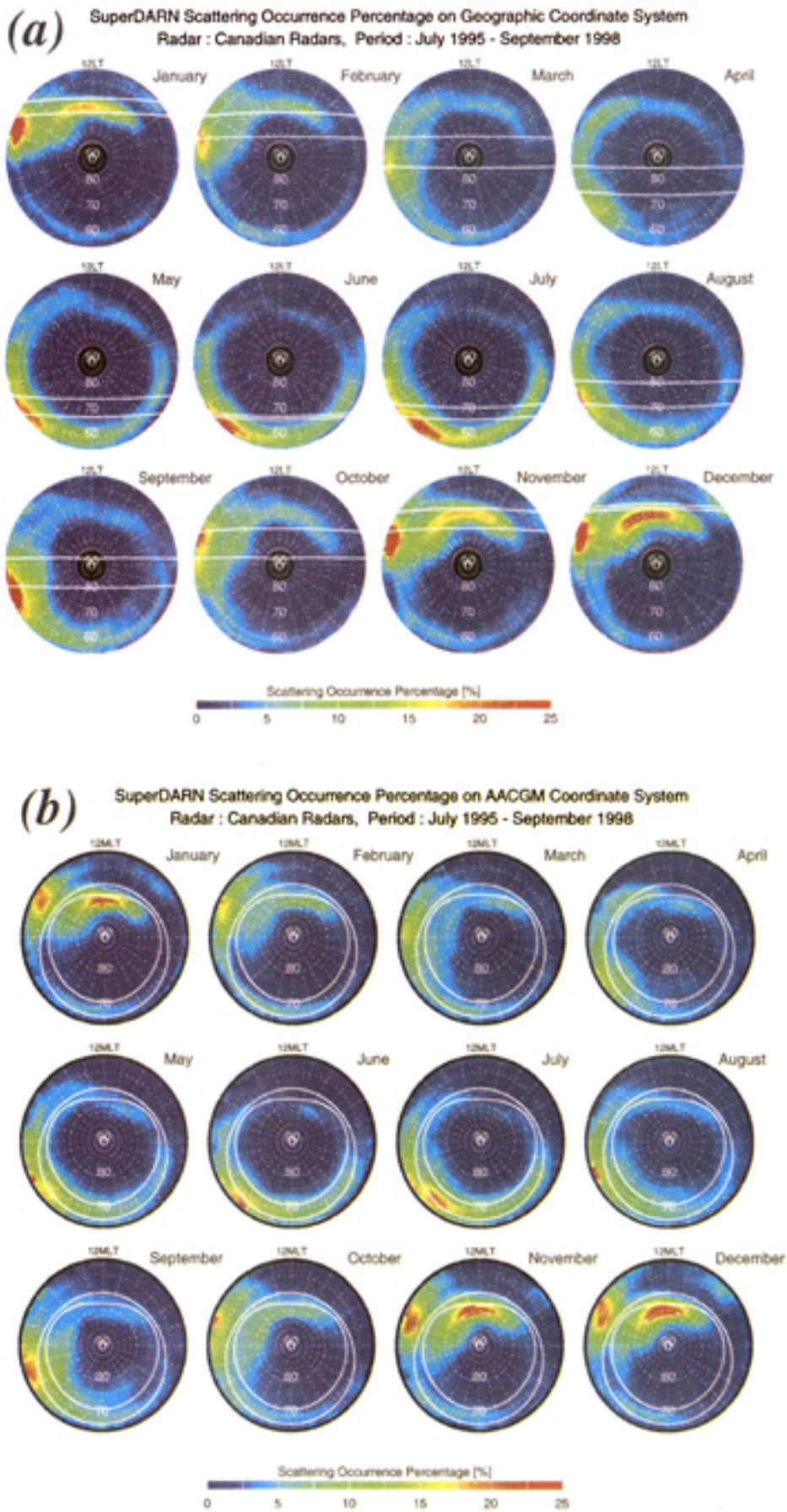

Plate 5. Monthly scattering occurrence percentage as a function of (a) geographic latitude and local time and (b) magnetic latitude and magnetic local time (AACGM coordinates).

According to the model of *Halcrow and Nisbet* [1977], the top and bottom limits of the sunrise wall (dawnside sunward edge) are specified in terms of the solar zenith angle:

$$\text{Top} \quad \text{SZA} = 87^\circ$$

$$\text{Bottom} \quad \text{SZA} = 95^\circ.$$

Here top means the point where depletion of plasma density starts; similarly, bottom means the point where the plasma density decrease ends. That is, sunward electron density gradient is considered to be strong between the top and the bottom of the sunward edge. In the case of sunset, the end of the trough is quite sensitive to magnetic activity. The sunset wall of the trough (duskside sunward edge of the trough) is prolonged far across the SZA 90° line during disturbed conditions. Hence it is necessary to incorporate a magnetic activity correction. Furthermore, the local time of the sunward edge is delayed by 1.5 hours compared with the dawnside:

$$\text{Top} \quad \text{SZA}(\text{LT} - 1.5) = 87^\circ - 3^\circ(Kp - 1/3)$$

$$\text{Bottom} \quad \text{SZA}(\text{LT} - 1.5) = 91^\circ - 3^\circ(Kp - 1/3).$$

The local time of the sunset edge predicted by this set of equations has to be delayed by 1.5 hours in practical use.

Plate 6 shows the monthly scattering occurrence profile of Canadian radars (Plate 6a) during quiet conditions ($0 \leq Kp \leq 1+$), (Plate 6b) during moderately disturbed conditions ($2- \leq Kp \leq 3+$), and (Plate 6c) during severely disturbed conditions ($4- \leq Kp \leq 9$). Here only the scattering occurrence percentages between 55° and 63° in geographic latitude are presented. Two white lines in each panel show the top and bottom of the sunward edge of the trough modeled by *Halcrow and Nisbet* [1977] where the Kp value is set to 0. In quiet conditions (Plate 6a), it is clearly seen that the peak of scattering occurrence lies in the region between the top and the bottom of the sunward edge of the trough in the dusk meridian for all months.

During moderately disturbed conditions (Plate 6b), we can find several characteristics which are not seen in quiet conditions. First, it is found that the area of higher occurrence extends to the dayside in all month periods. This signature is seen in both dawn and dusk sectors. The scale of the transition, however, is small in winter months (November, December, and January). Second, the center of the scattering occurrence peak shifts equatorward in all month periods. Especially in summer, the clear peak seems to escape to latitudes below the equatorward edge of the SuperDARN fields of view. In severely disturbed conditions (Plate 6c), the peak of scattering occurrence appears in earlier local time sectors. In addition, no clear peak of scattering occurrence is found in the periods except for winter months.

Halcrow and Nisbet [1977] and other papers treating the position of the trough [e.g., *Collis and Haggstrom*, 1988; *Rodger et al.*, 1992, and references therein] reported that the trough appears at lower latitudes with increasing local time in the dusk sector. Since dusk occurs at later local time sectors in summer, the intersection with the trough occurs at lower latitudes. Moreover, they indicated that the midlatitude trough shifts equatorward according to the motion of auroral oval during disturbed conditions. These characteristics of the trough indicate that the intersection of sunset and the midlatitude trough is located equatorward of the SuperDARN fields of view during disturbed conditions in summer. This is the reason why the strong DUSE signature disappears for disturbed conditions in summer. Furthermore, the occurrence percentage of the peak during disturbed conditions is enhanced in comparison with that in quiet conditions. For example, the occurrence percentage during disturbed conditions is 1.5 times of that during quiet conditions in the case of December. This increase may be due to the enhancement of plasma flow and associated electric field in disturbed conditions.

5. Discussion

5.1. Plasma Instabilities

Ionospheric FAIs are density fluctuations which have been amplified in plasma instability processes such as two-stream instability, current-convective instability, and gradient drift instability [*Fejer and Kelley*, 1980; *Keskinen and Ossakow*, 1983; *Tsunoda*, 1988]. At F region altitudes, the ion-neutral collision frequency is low; so ions and electrons move together with $\mathbf{E} \times \mathbf{B}$ drift velocity. Thus the two-stream instability is not generated in these altitudes. The current-convective instability is often employed to explain the generation mechanism of FAIs associated with particle precipitation and field-aligned currents. In the subauroral region, however, particle precipitation and field-aligned currents are not significant. Hence the gradient drift instability is considered to dominate the generation of FAIs in the subauroral F region.

A schematic diagram of gradient drift instability is described in Figure 2. If the plasma density gradient is directed in the y direction, an applied background electric field is in the x direction, and the geomagnetic field is in the $-z$ direction, the plasma is unstable and the geometry is favorable for the growth of the initial plasma density fluctuation. The linear growth rate of the density fluctuation γ is proportional to the plasma velocity V_0 and inversely proportional to the scale length of the background plasma density gradient, L; i.e., $\gamma \propto V_0/L$, where $V_0 = E_0/B$, $L = n_0/\nabla n_0$. B is the magnitude of the geomagnetic field, E_0 is the magnitude of the electric field in the plane perpendicular to $\mathbf{B}$, and n_0 is the background plasma density. Therefore when we estimate the formation process of FAIs based on the gra-

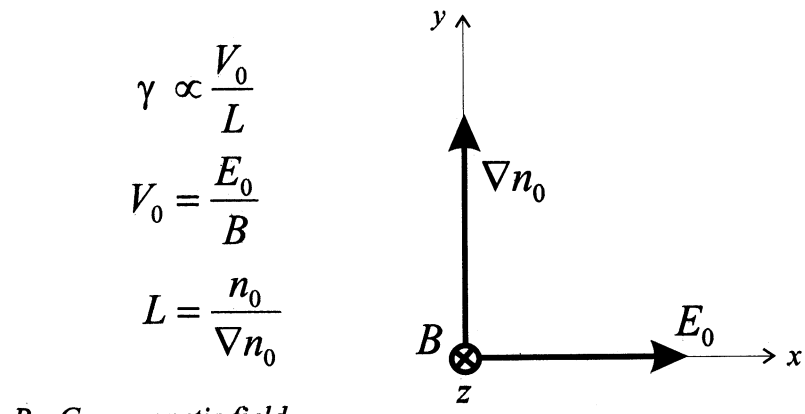

Figure 2. Schematic illustration of gradient drift instability.

dient drift instability, it is important to pay attention to the direction and amplitude of both the background electric field and the plasma density gradient.

5.2. Source Region of DUSE

If we consider the formation process of DUSE on the basis of the gradient drift instability, several models could be proposed. Here we set forth three models and discuss their possibility. Schematic illustrations of the models proposed here are summarized in Figure 3.

5.2.1. Model A. First, we consider only the plasma density gradient produced by solar EUV radiation and the ambient electric field. The EUV-related plasma density gradient is directed sunward around sunrise and sunset. *Ruohoniemi et al.* [1988] reported that the plasma velocity associated with DUSE is about 200 m/s, which consists of sunward (≈150 m/s) and poleward (≈50 m/s) components. Thus the ambient electric field is mainly directed poleward in this region. The relationship between ∇n_e and E_0 is illustrated in Figure 3 model A. In this scheme, the direction of the density gradient and the background electric field is favorable for the growth of FAIs. However, a plasma density gradient due to solar EUV exists at all latitudes of the polar ionosphere, which contradicts the fact that DUSE appears only at the intersection of sunset and the midlatitude trough. Moreover, the density gradient of solar EUV has no connection to the level of geomagnetic disturbance; so the dependence of the location of the DUSE echoes on the Kp index cannot be explained. Regarding the case of dawnside scatter event, solar EUV density gradient and dominant convective flow are again directed sunward, which is also favorable for the formation of FAIs. Statistical analysis, however, revealed that there exists a strong asymmetry of scattering occurrence between dawn and dusk. The reasons listed above would be enough to discount model A.

5.2.2. Model B. Next, we choose the density gradient at the poleward edge of the trough and small eastward electric field. The midlatitude trough has a steep poleward density gradient at its poleward edge. *Ruohoniemi et al.* [1988] reported that convective drift has a small poleward component (associated electric field directed eastward) in this region. The configuration of these parameters is illustrated in Figure 3 model B. In this case, the geometry is also favorable for the occurrence of gradient drift instability. *Ruohoniemi et al.* [1988] suggests the possibility that large-scale FAIs (more than 100 m) are generated in this process and damped into small-scale FAIs which can be observed by the SuperDARN radars. Statistical results, however, show that DUSE occurs within a few hours local time on the eveningside of sunset. If we assume that convective drift within the trough has a poleward component only around sunset, this mechanism can explain the localized appearance of DUSE. It is, however, difficult to consider that a poleward component of the convective flow is only seen where sunset occurs in the trough. Hence we suppose that this formation process cannot explain the statistical and observational results completely.

5.2.3. Model C. Finally, we propose another mechanism which has not been previously considered. Regarding our statistical results, the region where the DUSE occurs corresponds closely to the sunset edge of the midlatitude trough. The sunset edge of the trough

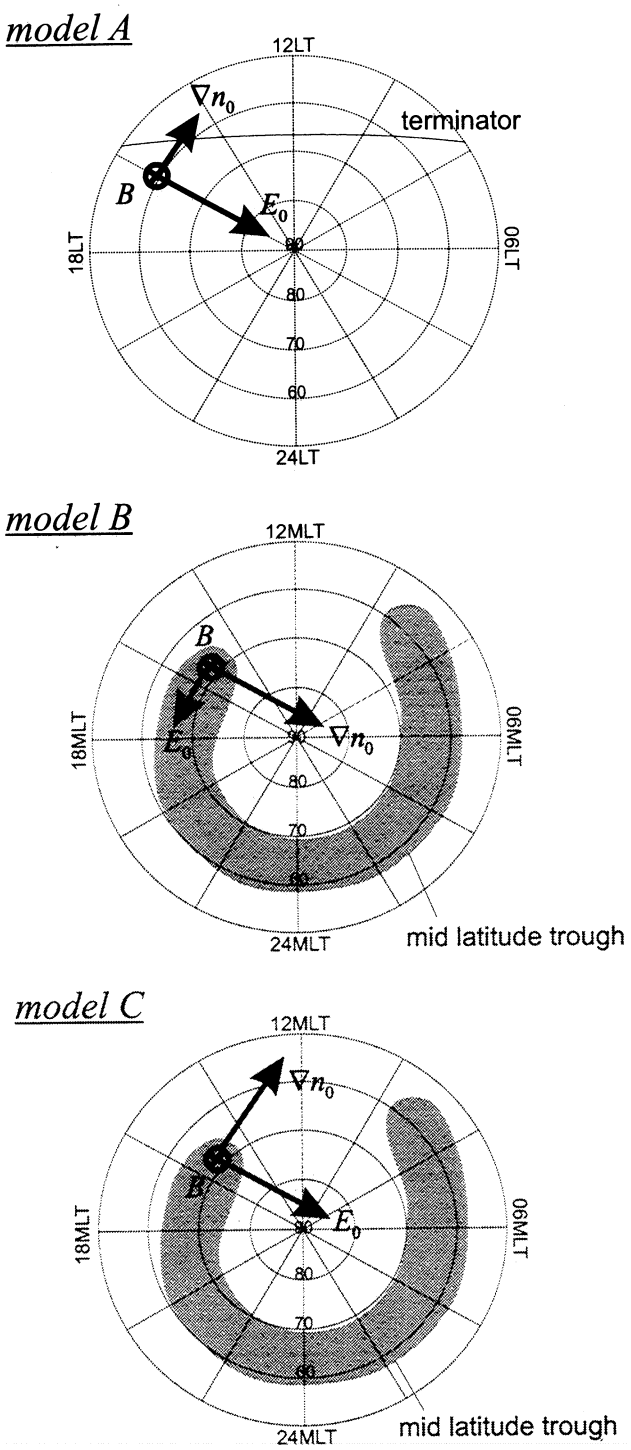

Figure 3. Schematic illustration of the possible formation mechanisms of DUSE based on the gradient drift instability.

has a steep plasma density gradient directed sunward. Assuming this density gradient and sunward plasma flow are dominant within the trough, the situation is also favorable for the growth of FAIs, which is described in Figure 3 model C. Since the plasma density gradient employed in this model exists only within the intersection of the midlatitude trough and sunset, this mechanism has no contradiction with the statistical results.

We found out several statistical results which support this model. Our statistical study shows that the DUSE in fact appears at earlier local times during disturbed conditions. *Halcrow and Nisbet* [1977] and *Whalen* [1989] pointed out that the sunward edge of the trough extends further into the dayside with increasing *Kp*. This trough feature was also reproduced by *Sojka et al.* [1990] using the Utah State University TDIM. Such characteristics of the trough can explain the *Kp* dependence of DUSE activity.

Furthermore, strong asymmetry in occurrence percentage between DUSE and DASE is identified in our statistics. There could be several factors creating this asymmetry. One is the difference in magnitude of the plasma density gradient between the sunrise and sunset edge of the trough. In fact, *Halcrow and Nisbet* [1977] indicated that the sunward plasma density gradient at the sunset edge of the trough is twice as sharp as that in the case of sunrise. The other is the difference in the occurrence of density gradient related to the trough wall between dawn and dusk. *Whalen* [1987] investigated the characteristics of the sunrise and the sunset edges of the trough using the global ionosonde network and reported that all ionosonde stations within a specific longitude range (110°W to 75°E) principally observed the density gradient associated with the sunset edge of the trough while sites outside this range mainly observed the density gradient at the sunrise edge of the trough. They suggested that this longitude dependence arose from the offset of the geomagnetic coordinate from the geographic coordinate. Since all radars used in the statistics are inside the longitude range they identified, this longitude dependence in the occurrence of density gradient could cause the occurrence asymmetry between DUSE and DASE.

Our statistical results exhibit a strong UT dependence such that the activity of DUSE (which is identical to occurrence percentage of DUSE) is more pronounced for universal times corresponding to dusk on the prime magnetic meridian (0° longitude). The modeling result by *Sojka et al.* [1990] demonstrates that the sunward directed density gradient at the sunset edge of the trough is steepest around the prime magnetic meridian (which corresponds to the eastern part of Canada). They showed that this dependence is also due to the offset between the geographic and geomagnetic poles. This longitude dependence of the density gradient is in good agreement with the UT dependence of DUSE activity as seen in our statistics.

5.3. Estimation of the Linear Growth Rate of FAIs

In this section, we estimate the linear growth rate of FAIs for all three mechanisms proposed in section 5.2 and determine which provides the most favorable conditions for the generation of FAIs. The linear growth rate of the plasma density fluctuation by the gradient drift instability has already been presented in section

5.1, which does not contain the effect of plasma diffusion. In practice, the growth of FAIs is opposed by plasma diffusion. The complete growth rate of FAIs by the gradient drift instability is

$$\gamma_c \propto \frac{V_0}{L} - k^2 D = \frac{E_0}{B} \cdot \frac{\nabla n_0}{n_0} - k^2 D,$$

where k is the wave number of FAIs, and D is the diffusion coefficient. Here we use the same diffusion coefficient as that used by *Ruohoniemi et al.* [1988] for comparison:

$$D = \frac{2k_B T_e \nu_{ei} m_e}{e^2 B^2}$$

where k_B is the Boltzmann constant and e, T_e, and m_e are the electron charge, temperature, and mass, respectively. Now we discuss the F region FAIs, and so the collision frequency between electrons and ions is considered [*Kelley*, 1989]:

$$\nu_{ei} = [34 + 4.18 \ln ({T_e}^2/n_e)] n_e {T_e}^{-3/2}.$$

These equations mean that if the complete growth rate γ_c is greater than zero, FAIs whose wave number equals k ($\lambda = 2\pi/k$ is equivalent to the scale of the FAIs) can grow by overcoming the diffusion effect. In short, large-scale FAIs are resistant to diffusion, and small-scale FAIs are easily diffused. Assuming γ_c is zero, we can obtain the maximum wave number, k_{max}, and associated minimum wavelength, λ_{min}, of the FAIs which can grow in this region. Backscatter of radar radio wave $\mathbf{k_r}$ occurs from FAIs with wave vector, $\mathbf{k}$, which satisfy the condition $\mathbf{k} = \pm 2\mathbf{k_r}$. Since the radar frequency is set anywhere from 8 to 20 MHz, the wavelength ($\lambda = 2\pi/2k_r$) of the FAIs which can be observed by the SuperDARN radar ranges from approximately 8 to 18 m. If the calculated minimum wavelength, λ_{min}, is shorter than 18 m, the SuperDARN radars can observe FAIs generated directly by the gradient drift instability.

In all models, the electron temperature T_e is set to 1.5×10^3 K as specified in the International Reference Ionosphere 1990 (IRI90) model [*Bilitza*, 1990], and the geomagnetic field B is 6.0×10^4 nT (from the International Geomagnetic Reference Field 2000 model). *Ruohoniemi et al.* [1988] reported that the plasma velocity associated width DUSE is about 200 m/s, which consists of sunward (≈150 m/s) and poleward (≈50 m/s) components. Hence we estimate the sunward convection velocity V_{sun} = 150 m/s and poleward velocity V_{pole} = 50 m/s. Assume that the plasma flows with the $\mathbf{E} \times \mathbf{B}$ drift velocity in this region; the associated electric fields are E_{pole} = 9.0 mV/m and E_{east} = 3.0 mV/m.

In model A, a background electron density, $n_e = 3.0 \times 10^{11}$ m^{-3}, and gradient, $\nabla n_e = 8.0 \times 10^4$ m^{-4}, are obtained from the IRI90 model. The calculated maximum wave number is $k_{max} = 0.017$ m^{-1} and minimum wavelength is $\lambda = 370$ m. Considering model B, we assume $n_e = 1.0 \times 10^{11}$ m^{-3} and $\nabla n_e = 1.3 \times 10^5$ m^{-4} at the poleward and sunset edge of the trough. These values are estimated from the result of *Halcrow and Nisbet* [1977]. As a result, $k_{max} = 0.049$ m^{-1} and $\lambda_{min} = 129$ m. In the last case, model C, input values are also obtained from the model of *Halcrow and Nisbet* [1977]: $n_e = 1.0 \times 10^{11}$ m^{-3} and $\nabla n_e = 2.4 \times 10^5$ m^{-4}. The result of the calculation is $k_{max} = 0.114$ m^{-1} and $\lambda_{min} = 54$ m. The results of the calculation are summarized in Table 2. It is found that the background condition of model C is most favorable for the growth of FAIs in this region. The calculated minimum wavelength, however, does not match the scale of FAIs observed by the SuperDARN radars even in model C. Small-scale FAIs tend to be generated by the electron density gradients at the edges of large-scale FAIs [*Tsunoda*, 1988], which causes the cascade process from large-scale FAIs into small-scale FAIs. Therefore it is suggested that this cascade process of FAIs is working also in the case of DUSE.

As claimed in the previous section, model C can explain the morphological features of DUSE completely. In particular, only this model can interpret the characteristics of DUSE during disturbed conditions, the asymmetry of FAI occurrence between sunrise and sunset, and the UT dependence of DUSE activity consistently. Estimation of linear growth rate of FAIs indicates that model C is most favorable for the growth of FAIs responsible for DUSE. Since the density gradient at the sunrise edge of the trough and the ambient plasma convection are directed sunward, the situation is basically the same in the case of dawn scatter event. Hence we can account for the appearance of DASE assuming the model C. Finally, we can conclude that the gradient drift instability that is driven by the sunward plasma density gradient at the sunward edge of the trough and the ambient poleward electric field is responsible for the localized enhancement of FAI occurrence around sunrise and sunset in the subauroral F region.

Table 2. Summary of the Estimated Parameters in Formation Models of DUSE

	n_0, m^{-3}	∇n_0, m^{-4}	L, m	V_0, m/s	E_0, mV/m	k_{max}, m^{-1}	λ_{min}, m
Model A	3.0×10^{11}	8.0×10^4	3750	150	9.0	0.017	370
Model B	1.0×10^{11}	1.3×10^5	770	50	3.0	0.049	129
Model C	1.0×10^{11}	2.4×10^5	416	150	9.0	0.114	54

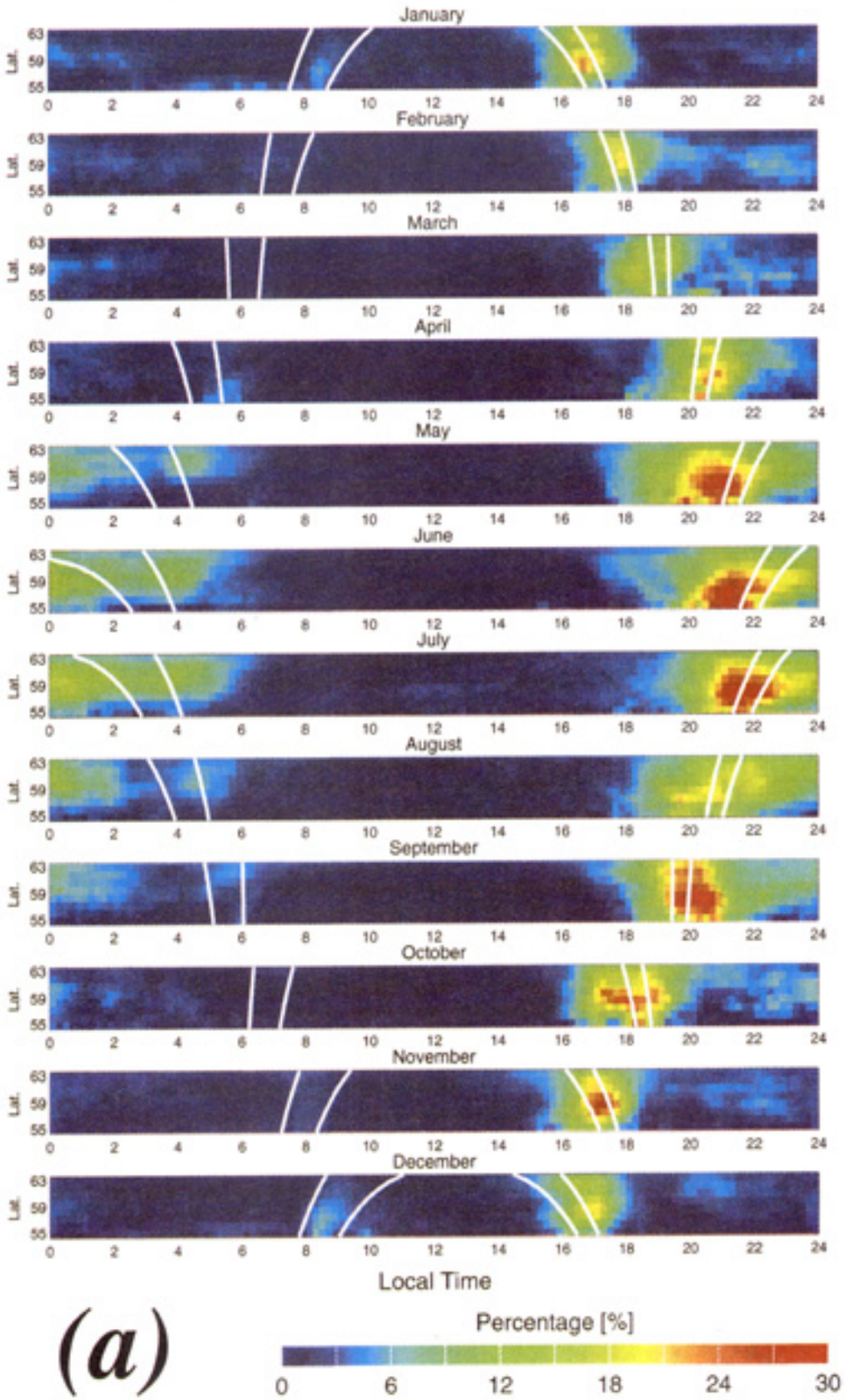

Plate 6. Monthly scattering occurrence percentage as a function of geographic latitude and local time during (a) quiet conditions ($0 \leq Kp \leq 1+$), (b) moderately disturbed conditions ($2- \leq Kp \leq 3+$) and (c) severely disturbed conditions ($4- \leq Kp \leq 9$). Two white lines indicate the top and bottom of the sunward edge of the midlatitude trough modeled by *Halcrow and Nisbet* [1977].

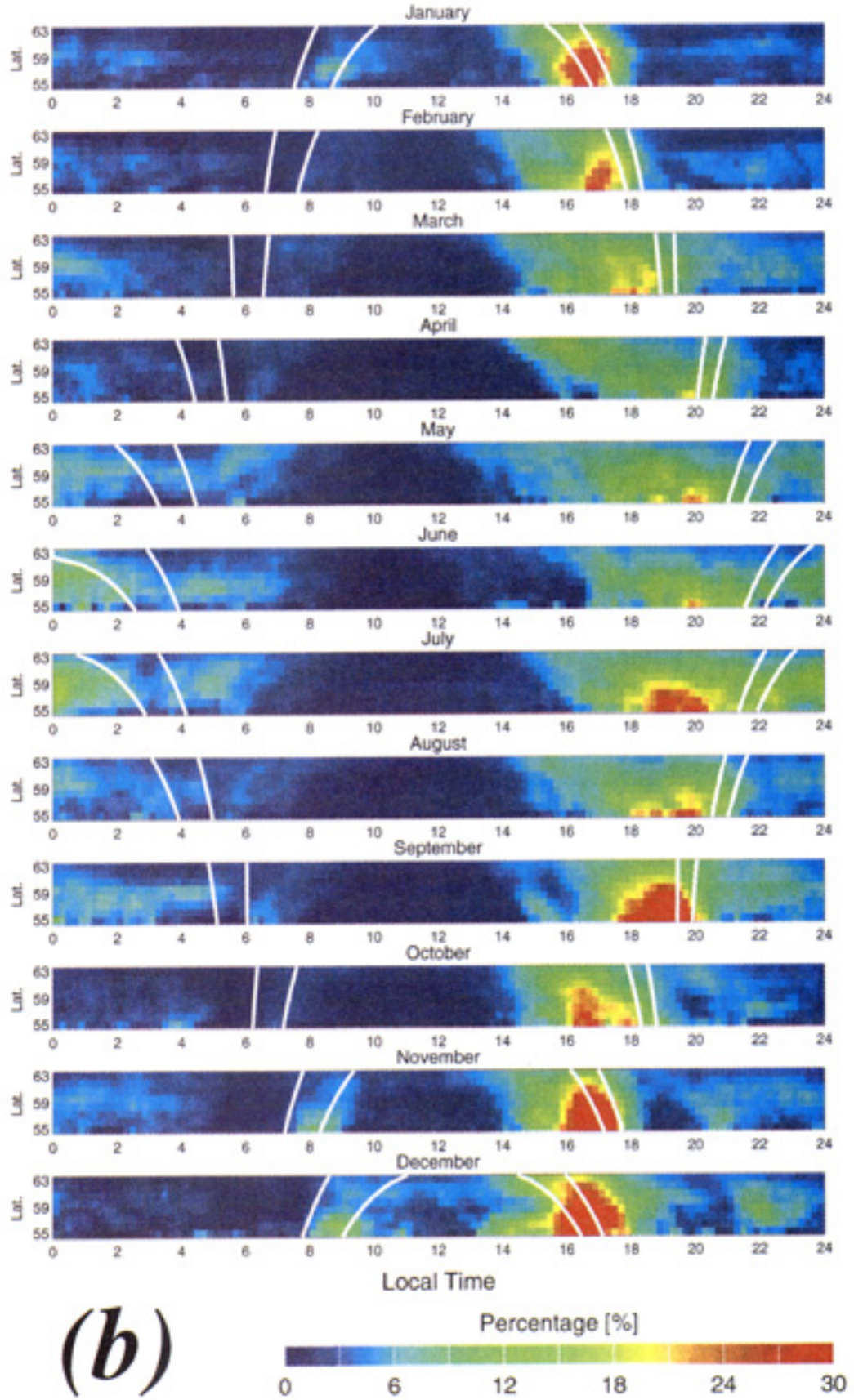

Plate 6. (continued)

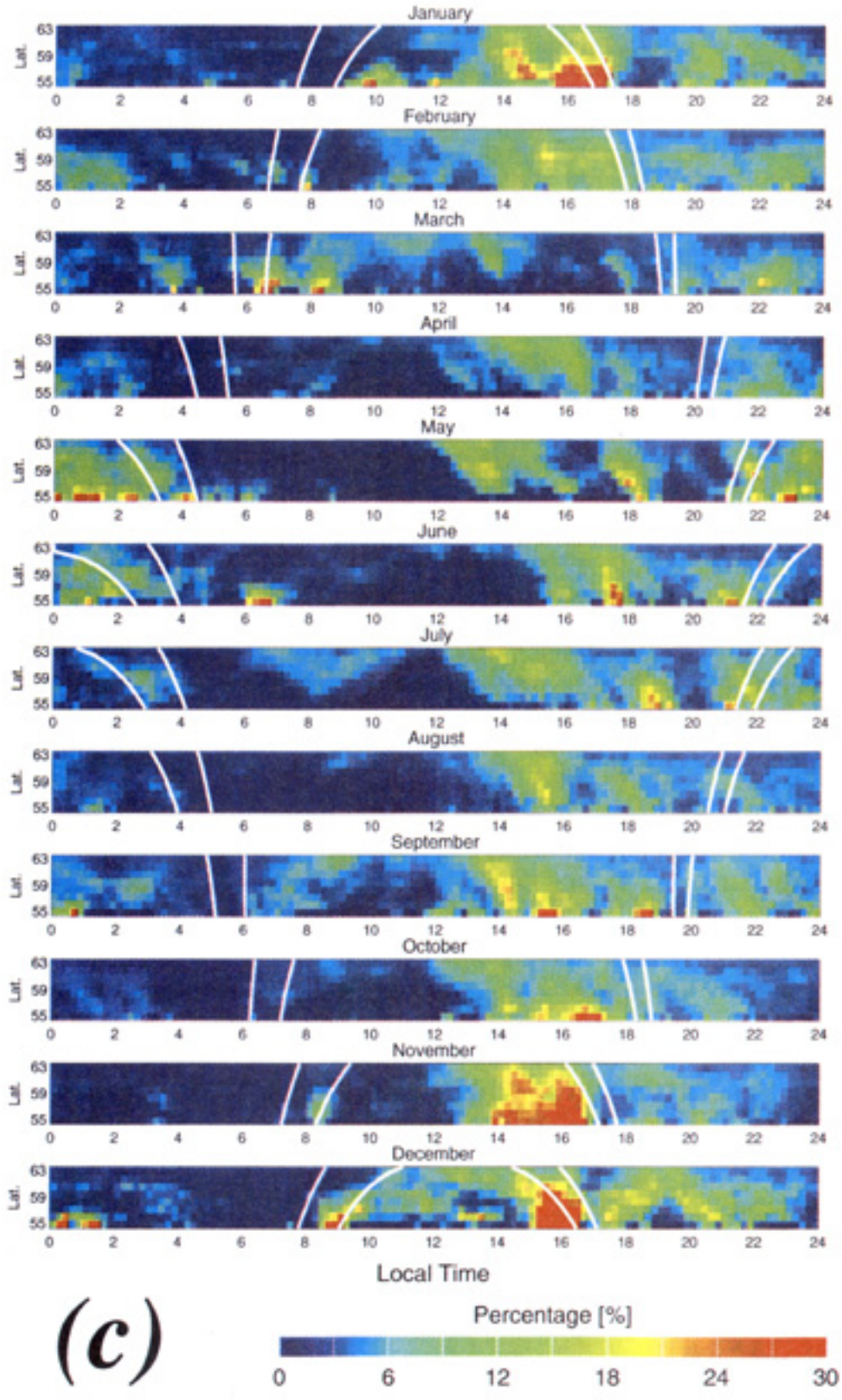

Plate 6. (continued)

6. Summary and Conclusion

In this paper, we investigated the scattering occurrence of the Northern Hemisphere SuperDARN radars and estimated the distribution of FAIs in the subauroral F region. We identified the morphological feature of the "dusk scatter event" (first reported by *Ruohoniemi et al.* [1988]) and clarified its relation to the boundaries of the plasma density in the subauroral F region.

The findings from this statistical analysis are as follows:

1. The statistical signature of DUSE can be found in the observations of the six Northern Hemisphere radars used in this study. The scale of DUSE ranges from 20° to 30° in longitude.

2. A peak in scattering occurrence percentage associated with DUSE is obtained throughout the year. DUSE is most clearly seen around the period centered on the summer and winter solstices.

3. There exists a clear UT effect in the characteristics of DUSE, such that activity of DUSE is more pronounced for universal times corresponding to dusk on the prime magnetic meridian (0° geomagnetic longitude), which is equivalent to the UT hours from 0100 to 0300 UT in summer and from 2200 to 2400 UT in winter.

4. An enhancement in scattering occurrence is also seen around sunrise (called "dawn scatter event"). Its percentage of scattering occurrence is rather small in comparison with that of DUSE; i.e., a clear asymmetry of FAI occurrence exists between sunrise and sunset.

5. The region where DUSE occurs is always located within a few hours of local time on the eveningside of the SZA 90° line and moves with the SZA 90° lines month by month.

6. In all months, the signature of DUSE appears on the dusk meridian where the magnetic latitude is slightly lower than the equatorward edge of the auroral oval, which corresponds to the plasma density depleted structure known as the midlatitude trough.

7. The region where DUSE appears has a close relationship with the sunset edge of the midlatitude trough modeled by *Halcrow and Nisbet* [1977]. The signature of DASE is also associated with the sunrise edge of the trough.

8. In disturbed conditions, the signature of DUSE appears at earlier local times compared with those of quiet conditions. In addition, the scattering occurrence percentage is considerably enhanced in disturbed conditions.

Three models based on the gradient drift instability were discussed. It was found that the model which is based on the sunward plasma density gradient at the sunward edge of the midlatitude trough and ambient poleward electric field (referred to as model C in the text) is most favorable for the explanation of DUSE appearance in this region. Consequently, we strongly suggest that DUSE and DASE are observed within the local time sectors where the sunward edges of the trough are located. This fact indicates that we can estimate the longitudinal extent of the midlatitude trough from the appearance of DUSE and DASE observed by SuperDARN, and this provides useful parameters for modeling the midlatitude trough. In order to test the consequences of the statistical analysis and model proposed in this paper, we are now investigating the simultaneous observation of the background parameters such as electric field, plasma density, and plasma temperature with both SuperDARN and the incoherent scatter radars during DUSE and DASE activity.

Acknowledgments. We thank all the staff who contributed to the operation of the SuperDARN radars, especially all PIs of Northern Hemisphere radars. The Goose Bay and Kapuskasing radars are operated under support from NSF grant ATM-9812078 and NASA grant NAG5-8361, respectively. Operation of the Saskatoon radar is supported by an NSERC CSPP grant for "The Canadian Component of SuperDARN". Operation of the Iceland West radar is supported by INSU of France. The Iceland-East/Finland radar pair (the Cooperative UK Twin Located Auroral Sounding System (CUTLASS)) is funded by the Particle Physics and Astronomy Research Council (UK) under grant PPA/R/R/1997/00256, the Finnish Meteorological Institute and the Swedish Institute for Space Research. This study is funded by a part of Ground Research for Space Utilization promoted by NASDA and the Japan Space Forum and also by grant 13640451 under Japan Society for Promotion of Sciences.

Hiroshi Matsumoto thanks J. M. Ruohoniemi and R. A. Greenwald for their assistance in evaluating this paper.

References

Baker, K. B., and S. Wing, A new magnetic coordinate system for conjugate studies of high latitudes, *J. Geophys. Res., 94,* 9139-9143, 1989.

Baker, K. B., R. A. Greenwald, J. M. Ruohoniemi, J. R. Dudeney, M. Pinnock, P. T. Newell, M. E. Greenspan, and C.-I. Meng, Simultaneous HF radar and DMSP observation of the cusp, *Geophys. Res. Lett., 17,* 1869-1871, 1990.

Baker, K. B., J. R. Dudeney, R. A. Greenwald, M. Pinnock, P. T. Newell, A. S. Rodger, N. Mattin, and C.-I. Meng, HF radar signatures of the cusp and low-latitude boundary layer, *J. Geophys. Res., 100,* 7671-7695, 1995.

Bilitza, D., International Reference Ionosphere 1990, *NSSDC/WDC-A-R&S 90-22,* Nat. Space Sci. Data Cent., World Data Cent. A for Rocket and Satell., Greenbelt, Md., 1990.

Collis, P. N., and I. Haggstrom, Plasma convection and auroral precipitation processes associated with the main ionospheric trough at high latitudes, *J. Atmos. Terr. Phys., 50,* 389-404, 1988.

Fejer, B. G., and M. C. Kelley, Ionospheric irregularities, *Rev. Geophys., 18,* 401-454, 1980.

Feldstein, Y. I., and G. V. Starkov, Dynamics of auroral belt and polar geomagnetic disturbance, *Planet. Space Sci., 15,* 209-229, 1967.

Greenwald R. A., K. B. Baker, R. A. Hutchins, and C. Hanuise, An HF phased-array radar for studying small-scale structure in the high-latitude ionosphere, *Radio Sci., 20,* 63-79, 1985.

Greenwald, R. A., et al., DARN/SuperDARN: A global view

of high-latitude convection, *Space Sci. Rev., 71,* 763-796, 1995.

Halcrow, B. W., and J. S. Nisbet, A model of F_2 peak electron density in the main trough region of the ionosphere, *Radio Sci., 12,* 815-820, 1977.

Hargreaves, J. K., and C. J. Burns, Electron content measurements in the auroral zone using GPS: Preliminary observations of the main trough and a survey of the degree of irregularity in summer, *J. Atmos. Terr. Phys., 58,* 1449-1457, 1996.

Holt, J. M., J. V. Evans, and R. H. Wand, Millstone Hill studies of the trough: Boundary between the plasmapause and magnetosphere or not?, *Radio Sci., 18,* 947-954, 1983.

Holzworth, R. H., and C.-I. Meng, Mathematical representation of the auroral oval, *Geophys. Res. Lett., 2,* 377-380, 1975.

Kelley, M. C., *The Earth's Ionosphere,* Academic, San Diego, Calif., 1989.

Keskinen, M. J., and S. L. Ossakow, Theories of high-latitude ionospheric irregularities: A review, *Radio Sci., 18,* 1077-1091, 1983.

Milan, S. E., T. K. Yeoman, M. Lester, E. C. Thomas, and T. B. Jones, Initial backscatter occurrence statistics from the CUTLASS HF radars, *Ann. Geophys., 15,* 703-718, 1997.

Milan, S. E., T. K. Yeoman, and M. Lester, The dayside auroral zone as a hard target for coherent HF radars, *Geophys. Res. Lett., 25,* 3717-3720, 1998.

Milan, S. E., M. Lester, S. W. H. Cowley, J. Moen, P. E. Sandholt, and C. J. Owen, Meridian-scanning photometer, coherent HF radar, and magnetometer observation of the cusp: A case study, *Ann. Geophys., 17,* 159-172, 1999.

Moffet, R. J., and S. Quegan, The mid-latitude trough in the electron concentration of the ionosphere F-layer: A review of observations and modeling, *J. Atmos. Terr. Phys., 37,* 161-167, 1983.

Rodger, A. S., R. J. Moffett, and S. Quegan, The role of ion drift in the formation of ionization troughs in the mid- and high-latitude ionosphere-A review, *J. Atmos. Terr. Phys., 54,* 1-30, 1992.

Rodger, A. S., S. B. Mende, T. J. Rosenberg, and K. B. Baker, Simultaneous optical and HF radar observations of the ionospheric cusp, *Geophys. Res. Lett., 22,* 2045-2048, 1995.

Ruohoniemi, J. M., and R. A. Greenwald, Statistical patterns of high-latitude convection obtained from Goose Bay HF radar observations, *J. Geophys. Res., 101,* 21,743-21,763, 1996.

Ruohoniemi, J. M., and R. A. Greenwald, Rates of scattering occurrence in routine HF radar observations during solar cycle maximum, *Radio Sci., 32,* 1051-1070, 1997.

Ruohoniemi, J. M., R. A. Greenwald, K. B. Baker, J. P. Villain, and M. A. McCready, Drift motions of small-scale irregularities in the high-latitude F region: An experimental comparison with plasma drift motions, *J. Geophys. Res., 92,* 4553-4564, 1987.

Ruohoniemi, J. M., R. A. Greenwald, J.-P. Villain, K. B. Baker, P. T. Newell, and C.-I. Meng, Coherent HF radar backscatter from small-scale irregularities in the dusk sector of the subauroral ionosphere, *J. Geophys. Res., 93,* 12,871-12,882, 1988.

Sojka, J. J., R. W. Schunk, and J. A. Whalen, The longitude dependence of the dayside F region trough: A detailed model-observation comparison, *J. Geophys. Res., 95,* 15,275-15,280, 1990.

Spiro, R. W., R. A. Heelis, and W. B. Hanson, Ion convection and the formation of the midlatitude F region ionization trough, *J. Geophys. Res., 83,* 4255-4264, 1978.

Tsunoda, R. T., High-latitude F region irregularities: A review and synthesis, *Rev. Geophys., 26,* 719-760, 1988.

Whalen, J. A., Daytime F layer trough observed on a macroscopic scale, *J. Geophys. Res., 92,* 2571-2576, 1987.

Whalen, J. A., The daytime F layer trough and its relation to ionospheric-magnetospheric convection, *J. Geophys. Res., 94,* 17,169-17,184, 1989.

Yeoman, T. K., M. Lester, S. W. H. Cowley, S. E. Milan, J. Moen, and P. E. Sandholt, Simultaneous observation of the cusp in optical, DMSP and HF radar data, *Geophys. Res. Lett., 24,* 2251-2254, 1997.

K. Hosokawa, Department of Geophysics, Graduate School of Science, Kyoto University, Kyoto 606-8502, Japan. (hosokawa@kugi.kyoto-u.ac.jp)

T. Iyemori, Data Analysis Center for Geomagnetism and Space Magnetism, Graduate School of Science, Kyoto University, Kyoto 606-8502, Japan. (iyemori@kugi.kyoto-u.ac.jp)

N. Sato and A. S. Yukimatu, National Institute of Polar Research, Itabashi-ku, Tokyo 173-8515, Japan. (nsato@nipr.ac.jp; sessai@uap.nipr.ac.jp)

(Received December 12, 2000; revised April 5, 2001; accepted May 15, 2001.)